

## Modeling of Porous Liner Using CE/SE Method with Application to Duct Aeroacoustics

George R. Hou<sup>1</sup>, Garret C. Y. Lam<sup>1</sup>, Randolph C. K. Leung<sup>1</sup> and Yves Aurégan<sup>2</sup>

<sup>1</sup>Department of Mechanical Engineering  
 The Hong Kong Polytechnic University, Hung Hom, Kowloon, Hong Kong, P. R. China

<sup>2</sup>Laboratoire d'Acoustique de l'Université du Maine  
 UMR CNRS 6613, Av. O Messiaen, F-72085 LE MANS Cedex 9, France

### Abstract

This paper proposes a new numerical modeling approach for porous liner with application to duct aeroacoustics which is different from classical impedance modeling of the lined surface. Direct aeroacoustic simulation (DAS) is adopted to describe the flow dynamics and acoustics inside porous liner by solving unsteady compressible Navier-Stokes equations with source terms that model the porous effect. Brinkman penalization method and Brinkman-Forchheimer-extended Darcy model are attempted to model the flow in porous medium. The single domain formulation eliminates the need to specify boundary conditions at fluid and porous interface explicitly. The in-house DAS code based on space-time conservation element and solution element (CE/SE) scheme is implemented to resolve low Mach number duct aeroacoustic problems with porous liner. The validation approaches and results are reported in this paper.

### Introduction

Noise pollution continues to be a crucial environment pollution. To enhance living comfort, adoption of porous liners is a common noise reduction approach. The liner is mostly placed on hard walls of a duct and the acoustic waves propagate along the wall under a grazing flow. Acoustic impedance is usually applied in modeling of a lined surface. Assuming that the flow is potential, wave equations in frequency domain with Ingard-Myers boundary condition [11] have been widely used in impedance modeling [2]. However, Renou and Aurégan [13] indicated the inadequacy of using this boundary condition in the presence of grazing flow because two different impedances were obtained for acoustics propagating in the flow direction and in the reverse direction respectively with experiment measurements. The detailed mechanism of acoustic behavior of porous liner in the presence of a grazing flow and the complex interaction between flow dynamics and acoustic field are still not clearly understood.

In this work, direct aeroacoustic simulation (DAS) is attempted to model the acoustics of porous liners. Such approach solves the unsteady compressible Navier-Stokes (N-S) equations and the equation of state to obtain the flow and acoustic fields simultaneously [7]. The effect of porous liner is treated as a source term in the N-S equations. Brinkman penalization method (BPM) and Brinkman-Forchheimer-extended Darcy model (BFDM) are adopted and compared to model the flow in porous medium. This approach is believed able to reveal the mechanism of noise reduction by porous liner under grazing flow. The aim of this paper is to report the ongoing work in validating this approach in application to duct aeroacoustics. To capture the acoustic behavior in DAS, the space-time conservation element and solution element (CE/SE) scheme [7] is implemented. This paper is organized as follows. The formulation of two selected models are illustrated first, followed by the numerical implementation of the two models including the

treatment of source terms in governing equations and the treatment of porous and nonporous interface. Then the validation approach and the result is demonstrated.

### Formulation

Generally, two dimensional aeroacoustic problems in porous liner under low Mach number flow are assumed. The porous liner is assumed as homogenous adiabatic porous material with constant porosity  $\phi$ . That way alleviates the exhaustive computational requirements for the calculation of flow dynamics near pores within porous liner. The conductivity in porous liner is assumed as the same as the fluid conductivity. The porous medium studied in the present study is saturated with air and assumed to be in local equilibrium. By choosing appropriate reference length  $\hat{L}_0$ , reference velocity  $\hat{u}_0$ , reference density  $\hat{\rho}_0$ , reference pressure  $\hat{p}_0 \hat{u}_0^2$ , reference viscosity  $\hat{\mu}_0$ , reference temperature  $\hat{T}_0$ , the normalized governing equation for two dimensional compressible flow can be written in the strong conservation form as

$$\frac{\partial U}{\partial t} + \frac{\partial(F - F_v)}{\partial x} + \frac{\partial(G - G_v)}{\partial y} = S \quad (1)$$

where

$$U = [\phi\rho, \phi\rho u, \phi\rho v, \phi\rho E]^T, \quad (2)$$

$$F = [\phi\rho u, \phi(\rho u^2 + p), \phi\rho uv, \phi(\rho E + p)u]^T, \quad (3)$$

$$G = [\phi\rho v, \phi\rho uv, \phi(\rho v^2 + p), \phi(\rho E + p)v]^T, \quad (4)$$

$$F_v = C_1 [0, \phi\tau_{xx}, \phi\tau_{xy}, \phi(\tau_{xx}u + \tau_{xy}v) - \phi q_x]^T, \quad (5)$$

$$G_v = C_1 [0, \phi\tau_{xy}, \phi\tau_{yy}, \phi(\tau_{xy}u + \tau_{yy}v) - \phi q_y]^T, \quad (6)$$

with  $E = \frac{p}{\rho(\gamma-1)} + \frac{u^2+v^2}{2}$ ,  $p = \frac{\rho T}{\gamma C_2}$ ,  $\tau_{xx} = \frac{2}{3}\mu(2\frac{\partial u}{\partial x} - \frac{\partial v}{\partial y})$ ,  $\tau_{xy} = \mu(\frac{\partial u}{\partial y} + \frac{\partial v}{\partial x})$ ,  $\tau_{yy} = \frac{2}{3}\mu(2\frac{\partial v}{\partial y} - \frac{\partial u}{\partial x})$ ,  $q_x = -\frac{\mu}{(\gamma-1)PrC_2}\frac{\partial T}{\partial x}$ ,  $q_y = -\frac{\mu}{(\gamma-1)PrC_2}\frac{\partial T}{\partial y}$ .  $S$  is a source term modeling the effect of porous material.  $\gamma$  is the ratio of specific heat  $\gamma = 1.4$ ,  $C_1 = 1/Re$  and  $C_2 = M^2$ , Reynolds number  $Re = \hat{\rho}_0 \hat{u}_0 \hat{L}_0 / \hat{\mu}_0$ ,  $M$  is Mach number  $M = \hat{u}_0 / \hat{c}_0$ ,  $\hat{c}_0 = \sqrt{\gamma \hat{R} \hat{T}_0}$ , the specific gas constant for air  $\hat{R} = 287.058 J / (kgK)$ , Prandtl number  $Pr = c_{p,0} \hat{\mu}_0 / \hat{k}_0 = 0.71$ . The dynamic viscosity  $\mu$  is calculated by Sutherland's Law,  $\mu = T^{\frac{3}{2}} (\frac{1 + \hat{S}_{su} / T_{su}}{\hat{T}_{su} + \hat{S}_{su} / \hat{T}_{su}})$ , where  $\hat{S}_{su} = 110.2^\circ C$  and  $\hat{T}_{su} = 20^\circ C$ . When taking acoustic speed  $\hat{c}_0$  as reference speed,  $C_1 = M/Re$  and  $C_2 = 1$ , the equations of  $p$ ,  $q_x$  and  $q_y$  are also replaced by  $p = \frac{\rho T}{\gamma}$ ,  $q_x = -\frac{\mu}{(\gamma-1)Pr} \frac{\partial T}{\partial x}$  and  $q_y = -\frac{\mu}{(\gamma-1)Pr} \frac{\partial T}{\partial y}$ . It is noted that all velocity variables in governing equations are intrinsic fluid velocity instead of Darcy velocity.

The formulation of BFDM is derived referring to previous study on flow dynamics in porous media [15]. Darcy term and Forchheimer term are put at the right hand side of equation 1 as source terms. Brinkman term was placed at left hand side equation since it is analogous to the shear stress terms in the N-S equations by replacing  $\mu$  by effective viscosity  $\tilde{\mu} = \mu/\phi$  [12]. The normalized source term of the formulation of BFDM can be written as

$$S = S_{BFDM} = \begin{bmatrix} 0 \\ -\phi^2 \frac{\mu}{Re} \frac{1}{Da} u - \frac{F\rho\phi^3}{\sqrt{Da}} u\sqrt{u^2+v^2} \\ -\phi^2 \frac{\mu}{Re} \frac{1}{Da} v - \frac{F\rho\phi^3}{\sqrt{Da}} v\sqrt{u^2+v^2} \\ -[\phi^3 \frac{\mu}{Re} \frac{1}{Da} (u^2+v^2) + \frac{F\rho\phi^4}{\sqrt{Da}} (u^2+v^2)^{\frac{3}{2}}] \end{bmatrix}, \quad (7)$$

where Darcy number  $Da = \hat{K}/\hat{L}_0^2$ ,  $\hat{K}$  is permeability of porous material,  $F$  is Forchheimer coefficient. The first and the second terms in the source term is normalized Darcy term and Forchheimer term respectively.

#### BPM for Two Dimensional Compressible Flow

Liu and Vasilyev [8] propose Brinkman penalization method for calculating compressible flows in porous medium. This method adopts Brinkman penalization terms  $-\frac{\Psi}{\alpha}u$  and  $-\frac{\Psi}{\alpha_T}(T-T_p)$  in momentum and energy equation as new simplified source terms to replace Brinkman term, Forchheimer term and Darcy term. They argue that similar to the original terms, the penalization terms results in significant damping of the momentum inside of porous medium and satisfying the no-slip boundary condition at the solid surface. The normalized source term of BPM can be written as [8]

$$S = S_{BPM} = [0, -\frac{\Psi}{\alpha}u, -\frac{\Psi}{\alpha}v, -\frac{\Psi}{\alpha_T}(T-T_p)]^T, \quad (8)$$

where  $\begin{cases} \Psi_{(x,y,t)} = 1, & x,y \in O_i \\ \Psi_{(x,y,t)} = 0, & otherwise \end{cases}$ .  $T_p$  is porous medium's normalized temperature which is assumed to be as the same as  $T$ ,  $O_i$  indicates the porous medium,  $\alpha$  and  $\alpha_T$  are penalization coefficients which are adjustable. However, the determination of  $\alpha$  and  $\alpha_T$  was not discussed in Liu and Vasilyev [8].

#### Numerical Implementation

##### Space-time CE/SE Scheme for N-S Equations

To solve the governing equations, CE/SE method with treatment of source term is adopted in our in-house code. CE/SE is a high-resolution scheme emphasizes on strict flux conservation and the unified treatment in both space and time with non-dissipative characteristics which meets the requirement of low Mach number DAS that the widely disparate flow and acoustic scales can be solved with uniform numerical accuracy. The detailed description of CE/SE method and boundary conditions implementation are referred to [7].

##### Treatment of Source Terms

Newton's iterative method is applied to treat the stiff source term [9]. A Newton iterative procedure to calculate  $U$  can be expressed as

$$U^{(i+1)} = U^{(i)} - \left(\frac{\partial\Phi}{\partial U}\right)^{-1}[\Phi(U^{(i)}) - U_H], \quad (9)$$

where  $i$  is the iteration number,  $\Phi(U) = U - S(U)\Delta t$ ,  $S$  is the source term in the governing equations which is a function of  $U$ ,  $U_H$  is the homogeneous solution ( $S = 0$ ). The quantities  $\left(\frac{\partial\Phi}{\partial U}\right)^{-1}[\Phi(U^{(i)}) - U_H]$  are calculated by applying Cramer's rule to update  $U^{(i+1)}$  from  $U^{(i)}$ . The convergence criterion is set as the maximum difference value among solution vectors of two adjacent iteration values reaches  $10^{-30}$ .

##### Treatment of Interface between Fluid and Porous Material

At the interface between porous and nonporous area, there is a sudden change of the flux due to the porosity difference between porous and nonporous region. Mößner and Radespiel [10] adopted a fictive cell concept to successfully overcome their pressure jump problem at the porous-nonporous interface in their solver. The sudden change of the flux at the interface can also be solved by using fictive cell method. In CE/SE method, the porous cell is converted to a fictive nonporous cell where the solutions are equal to those in the porous cell divided by the porosity  $\phi$  of the porous material. The fluxes into the nonporous cell are then calculated by using the solutions of the newly created fictive nonporous cell. On the other hand, the nonporous cell is converted to a fictive porous cell and compute the flux into the porous cell using the solutions multiplied by the porous material porosity  $\phi$ . It is noted that the spatial and time gradients of the solution values are also calculated by applying fictive cell method.

#### Validation

The validation of the numerical modeling was divided into three stages with different levels of complexity. In the first stage, its capability on simulating flow dynamics in porous material was examined. It was tested by two benchmark cases. The first test case (Test I) is a uniform flow through a homogeneous porous medium under given pressure gradient with sliding walls. Afterwards, the performance of the model on simulating flow at porous and fluid interface was then examined by an experimental investigation on the transition layer thickness at a fluid-porous interface (Test II) [4]. In the second stage, the capability of the model in capturing acoustic fields was examined by an experiment investigating acoustic behavior of a homogeneous porous material (Test III) [3]. In the third stage, the capability of the model in capturing the interactions between the aerodynamic and acoustic fields will be examined by investigating acoustic behavior of a homogeneous porous material under grazing flow [3]. The validity of the numerical model will be established when it passes all the above tests. The third stage of the validation is still in progress.

##### Test I: Uniform Flow in Porous Medium

The height of the porous medium  $\hat{H} = 0.01m$  was chosen as the reference length. The computation domain is  $20 \times 1$  with mesh size  $\Delta x = 0.05$  and  $\Delta y = 0.02$ . Non-reflecting boundary condition was set at the outlet. Mach number was  $M = 0.002$ . The porosity of the porous medium  $\phi$  was 0.6. The reference density and reference viscosity was set by the air density and air viscosity respectively,  $\hat{\rho}_0 = 1.225kg/m^3$ ,  $\mu_0 = 1.795 \times 10^{-5}kg/m \cdot s$ . Reynolds number  $Re_H = 465.363$ . For BPM, adjustable parameter  $\alpha$  and  $\alpha_T$  was set as 0.01 based on Liu and Vasilyev's work [8]. For BFDM, Darcy number  $Da = 0.004$ ,  $F = 0.002$ . Initially full field velocity was set to be uniform.

Under incompressible flow assumption, for BPM, the steady fully developed fluid motion in the porous medium is governed by

$$\frac{dp}{dx} = -\frac{\Psi}{\eta}u. \quad (10)$$

For BFDM, the steady fully developed fluid motion in the porous medium is governed by

$$\frac{dp}{dx} = -\phi \frac{\mu}{Re Da} u - \frac{F \rho \phi^2}{\sqrt{Da}} u^2. \quad (11)$$

The flow is supposed to keep the uniform velocity profile when the pressure gradient set for simulations balances the penalty terms in BPM and the sum of Darcy term and Forchheimer term in BFDM.

As shown in figure 1, the velocity along  $x$  direction  $u$  of check point calculated by BFDM becomes steady and is very close to analytical solution. The relative error of  $u$  is within the range from  $-5 \times 10^{-4}\%$  to  $9 \times 10^{-4}\%$ . The numerical results of pressure and pressure gradient also show agreement with analytical solution. The relative error of pressure is within the range between  $-2 \times 10^{-5}\%$  and  $1 \times 10^{-5}\%$ .

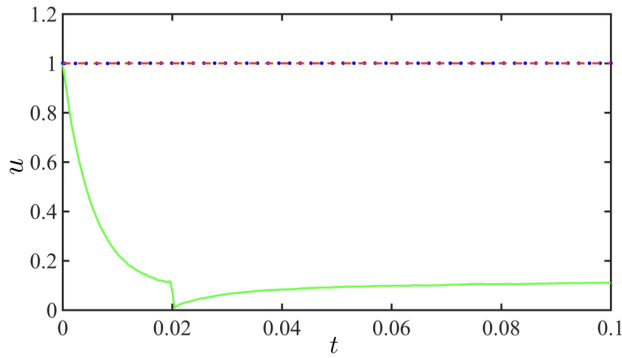


Figure 1: Variation of velocity  $u$  along time at the center of the domain. The red dashed line shows the analytical solution. The blue dots show the numerical result calculated by BFDM. The green solid line shows the numerical solution calculated by BPM.

For BPM, the velocity along  $x$  direction  $u$  drops quickly from initial condition 1 to around 0.1. This result may be influenced by the determination of adjustable parameters  $\alpha$  and  $\alpha_T$ . Since there is no discussion on the determination of  $\alpha$  and  $\alpha_T$  in literature, BPM was not further adopted in this research.

#### Test II: Flow at a Fluid-Porous Interface

Figure 2 shows the numerical settings of the computation domain which follows the experimental setup used by Goharzadeh et al. [4]. The third glass beads sample (GB3) was selected as the porous material in the simulation. The parameters of porous material and flow used in computation follow the settings in that experiment: the porosity of the porous medium  $\phi = 0.41$ , the average particle diameter  $\hat{d}_p = 0.65\text{cm}$ , the height of the fluid layer  $\hat{H}_f = 4\text{cm}$ , Reynolds number  $Re_{H_f} = 21$ . The maximum flow velocity at the fluid surface along  $x$  direction  $\hat{u}_{max}$  and  $\hat{H}_f$  were chosen as reference length and reference velocity. The transition layer thickness which is defined by the height below the permeable interface up to where the velocity decreases to the Darcy scale and the porosity variation in the transition layer was set derived on the data in their work [4]. The permeability was calculated based on Carman-Kozeny equation [1],  $K = \frac{d_p^3 \phi^3}{180(1-\phi)^2}$ . Forchheimer coefficient  $F = 0.1076$  was estimated by the empirical equation [1],  $F = 0.55(1 - 5.5 \frac{d_p}{D_e})$ , where  $De$  is defined in terms of the height  $h_p$  and width  $w_p$  of the porous material by  $De = \frac{2w_p h_p}{w_p + h_p}$ .

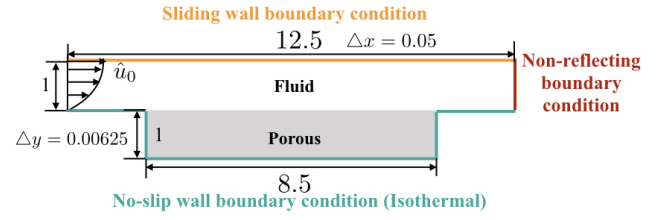


Figure 2: Schematic view of the channel flow with porous medium

The comparison of present numerical result with experimental data measured by Goharzadeh et al. [4] and other results from literature [5, 14] is shown in figure 3. The current model with the porous and fluid interface treatment using fictive cell concept [10] matches the experimental data best. This shows that the proposed approach can accurately capture the flow behavior in both fluid and porous region as well as at their interface. Therefore, the present porous model passes the first stage of the validation successfully.

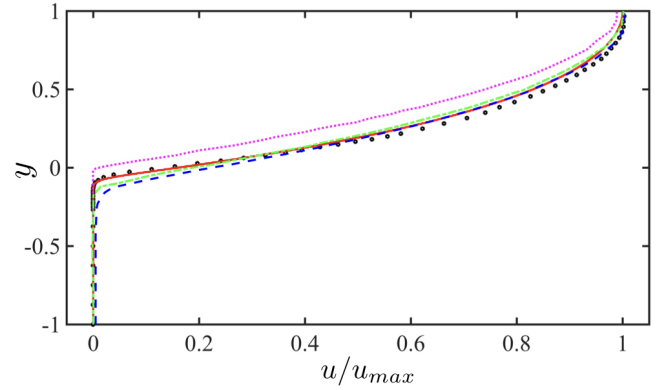


Figure 3: Velocity profile along the cross section at the center of the domain. The black dots are experimental values [4]. The red solid line shows present numerical result. The magenta dotted line shows the numerical result calculated by Gualtieri [5]. The green dash-dot line shows the analytical solution with linearly variable porosity,  $C=18$ , obtained by Tao et al. [14]. The blue dashed line shows the analytical solution with exponentially variable porosity obtained by Tao et al. [14].

#### Test III: Acoustics Fields in Porous Liner

The computation domain (figure 4) follows the experimental setup conducted by Aurégan et al [3]. A uniform mesh with  $\Delta x = 0.05$  and  $\Delta y = 0.01$  was set between  $-50 < x < 63.3$ . There were total 50 elements in each buffer zone stretched exponentially along  $x$  direction with maximum  $\Delta x = 76$  and minimum  $\Delta x = 0.05$ . The parameters of porous liner and duct used in computation follows the experiment: the porosity of the metallic foam  $\phi = 0.9$ , resistivity of metallic foam  $\hat{\sigma} = 6900\text{kgm}^{-3}\text{s}^{-1}$ , height of the duct  $\hat{h} = 15\text{mm}$ . Duct height  $\hat{h}$  and acoustic speed  $\hat{c}_0$  were selected as reference length and reference velocity. Reynolds number  $Re_h = 349022.346$ . Darcy number  $Da = \frac{K}{\hat{h}^2} = \frac{\hat{h}}{\hat{\sigma} \hat{h}^2} = 1.153 \times 10^{-5}$ , Forchheimer coefficient  $F = 0.520$ . The acoustic excitation was set at  $x = -50$  with a broadband frequency that corresponds to a range from 100 Hz to 3000 Hz with increment of 5 Hz in experiment. The amplitude of the acoustic pressure was set as  $8.208 \times 10^{-7}$ . Acoustic transmission and reflection coefficients of the lined

part were calculated based on the optimized multiple microphone method proposed by Jang et al. [6]. Check points were set at the center line of the duct from  $x = -21$  to  $x = -3$  and from  $x = 16.3$  to  $x = 34.3$  with increment of 3.

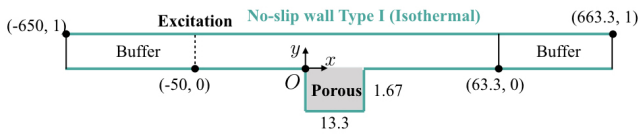


Figure 4: Schematic view of the computation domain

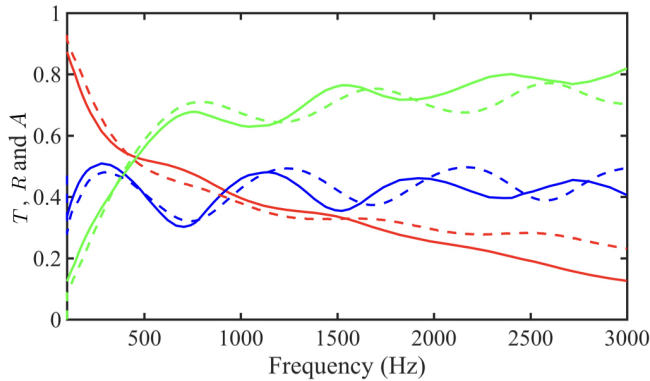


Figure 5: Absolute value of the transmission coefficients  $T$  (red) and reflection coefficients  $R$  (blue) and absorption coefficient  $A$  (green) of the porous liner. The dashed lines are numerical results and solid lines are experimental values in [3].

As shown in figure 5, numerical result shows agreement with experiment result at low frequency range from 100 Hz to 1500 Hz. A finer mesh with  $\Delta x = 0.02$  between  $-50 < x < 63.3$  was used to simulate and the result has no obvious difference from the one showed above. The discrepancy and shift may be caused by the difference between the two dimensional and homogeneous porous material assumption of the modeling and the experiment will be further studied. The present porous model has the capability in capturing acoustic fields of duct lined with porous liner. Thus, the proposed approach has been successfully validated in the second stage.

## Conclusions

In this paper, a new modeling approach of porous liner with application to duct aeroacoustics using CE/SE method is introduced and successfully validated. The proposed single domain formulation using Brinkman-Forchheimer-extended Darcy model (BFDM) can accurately calculate the flow dynamics and acoustics in both fluid and porous region as well as at their interface. The validation on the capability of the model in capturing the interactions between the flow dynamics and acoustics, i.e. the acoustic behavior of porous liner under grazing flow, will be carried out in the future.

## Acknowledgements

The authors gratefully acknowledge the support from ANR/RGC Joint Research Scheme of the Research Grants Council of Hong Kong SAR Government under Grant No. A-PolyU503/15 and the ANR/RGC international project FlowMatAc No. ANR-15-CE22-0016-01. The third author gratefully acknowledges the support with a research donation from Philip K. H. Wong Foundation under Grant No. 5-ZH1X.

## References

- [1] A.Nield, D. and Bejan, A., *Convection in Porous Media*, 2010, 3rd edition.
- [2] Aurégan, Y., Leroux, M. and Pagneux, V., Measurement of Liner Impedance with Flow by an Inverse Method, in *10th AIAA/CEAS Aeroacoustics Conference*, American Institute of Aeronautics and Astronautics, Reston, Virginia, 2004.
- [3] Aurégan, Y. and Singh, D. K., Experimental observation of a hydrodynamic mode in a flow duct with a porous material., *The Journal of the Acoustical Society of America*, **136**, 2014, 567–72.
- [4] Goharzadeh, A., Khalili, A. and Jørgensen, B. B., Transition layer thickness at a fluid-porous interface, *Phys. Fluids*, **17**, 2005, 057102.
- [5] Gualtieri, C., Numerical simulation of transition layer at a fluid-porous interface, in *5th International Congress on Environmental Modelling and Software*, Ottawa, Ontario, Canada, 2010, 230–242, 230–242.
- [6] Jang, S. H. and Ih, J. G., On the multiple microphone method for measuring in-duct acoustic properties in the presence of mean flow, *J. Acoust. Soc. Am.*, **103**, 1998, 1520–1526.
- [7] Lam, G. C. Y., Leung, R. C. K., Seid, K. H. and Tang, S. K., Validation of CE / SE Scheme in Low Mach Number Direct Aeroacoustic Simulation, *Int. J. Nonlinear Sci. Numer. Simul.*, **15**, 2014, 157–169.
- [8] Liu, Q. and Vasilyev, O. V., A Brinkman penalization method for compressible flows in complex geometries, *J. Comput. Phys.*, **227**, 2007, 946–966.
- [9] Loh, C. Y. and M. Q. Zaman, K. B., Numerical Investigation of Transonic Resonance with a Convergent-Divergent Nozzle, *AIAA Journal*, **40**, 2002, 2393–2401.
- [10] Mößner, M. and Radespiel, R., Modelling of turbulent flow over porous media using a volume averaging approach and a Reynolds stress model, *Comput Fluids*, **108**, 2015, 25–42.
- [11] Myers, M., On the acoustic boundary condition in the presence of flow, *J. Sound Vib.*, **71**, 1980, 429–434.
- [12] Ochoa-Tapia, J. A. and Whitaker, S., Momentum transfer at the boundary between a porous medium and a homogeneous fluid-I. Theoretical development, *International Journal of Heat and Mass Transfer*, **38**, 1995, 2635–2646.
- [13] Renou, Y. and Aurégan, Y., Failure of the IngardâMyers boundary condition for a lined duct: An experimental investigation, *The Journal of the Acoustical Society of America*, **130**, 2011, 52–60.
- [14] Tao, K., Yao, J. and Huang, Z., Analysis of the laminar flow in a transition layer with variable permeability between a free-fluid and a porous medium, *Acta Mech.*, **224**, 2013, 1943–1955.
- [15] Tasnim, S. H., Mahmud, S., Fraser, R. A. and Pop, I., Brinkman-Forchheimer modeling for porous media thermoacoustic system, *Int. J. Heat Mass Transfer*, **54**, 2011, 3811–3821.